

Research Article

Influence of Water Injection Pressure on Methane Gas Displacement by Coal Seam Water Injection

Tianwei Shi ¹, Yishan Pan ^{1,2}, Wenhong Zheng ¹ and Aiwen Wang ^{1,2}

¹School of Mechanics and Engineering, Liaoning Technical University, Fuxin 123000, China

²School of Environment, Liaoning University, Shenyang 110036, China

Correspondence should be addressed to Tianwei Shi; tangzhi@lntu.edu.cn and Aiwen Wang; waw_lgd@126.com

Received 23 August 2022; Accepted 14 September 2022; Published 28 September 2022

Academic Editor: Jianchao Cai

Copyright © 2022 Tianwei Shi et al. This is an open access article distributed under the Creative Commons Attribution License, which permits unrestricted use, distribution, and reproduction in any medium, provided the original work is properly cited.

It is of great significance to study the pattern of displacing methane gas with water in the coal seam water injection process for the prevention and control of gas disasters. A two-phase displacement test device was used to conduct experiments on the water injection of coal samples to displace methane gas under different water injection pressures, and the influence of the water injection pressure on the displacement was analyzed. The test results show that with the same displacement time, the ratio of displaced methane increases with the increase in the water injection pressure. The displacement rate increases with the increase in the water injection pressure at the stage without water discharge, while the water displacement rate under different water injection pressures differed slightly; in the later displacement stage, a higher water injection pressure of the coal sample results in a faster attenuation of the displacement rate and water displacement rate due to the decrease in the methane content in the coal sample. There is a critical water injection pressure to displace methane gas. When the critical water injection pressure is exceeded, the displacement time does not change appreciably. Flowing water can displace a large amount of methane gas in coal, and the methane displacement rate increases with the increase in the water injection pressure. The high solubility of methane in water is the reason for the high methane displacement rate. The results of this study can provide theoretical guidance for coal seam water injection to control gas disasters.

1. Introduction

Gas is a hazardous source threatening coal mine safety production. According to statistics, from 2008 to 2020, the number of deaths caused by gas disasters in China's coal mines accounted for 33% of the total number of deaths in coal mines. Gas disasters are the most fatal coal mine disasters, and coal and gas outbursts are the most serious types of gas disasters [1]. Coal and gas outbursts are the result of the combined effect of three factors, i.e., gas, crustal stress, and coal physical and mechanical properties [2–4]. Therefore, reducing the coal seam stress and changing the physical and mechanical properties of coal and gas desorption characteristics are effective ways to control coal and gas outbursts.

Coal seam water injection has various modification effects on coal seams. After wetting, the physical and mechanical parameters of the coal body, such as the uniaxial

compressive strength, elastic modulus, brittleness, and the ability to accumulate elastic energy, decrease, while the plasticity increases [5–9]. The changes in the coal physical and mechanical properties reduce the stress concentration of the coal body in front of the mining face [10, 11]. The water entering the coal seam reduces the gas desorption rate and desorption capacity by blocking the gas diffusion and seepage channels [12, 13]. Many scholars consider coal seam water injection as an effective measure to prevent coal and gas outbursts, and this measure has been widely used in many countries [14–17].

Studies have shown that the replacement of methane molecules adsorbed on the coal surface by water molecules is an exothermic process, indicating that the ability of coal to adsorb water molecules is stronger than its ability to adsorb methane molecules [18]. Extensive laboratory experiments have confirmed that the water injected into the coal body can displace the adsorbed methane gas [19–26]. At

the coal seam water injection site, some wet areas have reduced gas content, and other wet areas have increased gas content in the coal body, and the elevated gas content increases the risk of gas hazards. This phenomenon, which causes a change in the distribution of gas content, is thought to be caused by the displacement of methane gas by water [18, 27]. However, there is a lack of support by experimental data.

Water displacement in coal seam water injection also has a favorable role. In gas extraction projects, the properties of coal with different adsorption strengths toward different gases have been utilized to replace a weakly adsorbed gas with a strongly adsorbed gas in the coal body, so that the weakly adsorbed gas becomes free gas, which is then extracted from the coal body. Hence, an increase in production can be achieved by gas injection, which is one the mechanism for promoting enhanced coalbed methane (ECBM) recovery [28–30]. According to the principle of ECBM recovery, coal seam water injection can also be used for gas extraction to improve the prevention and control of coal seam gas disasters.

The above analysis reveals that water displacement can both hurt and help the prevention and control of gas disasters. Understanding the pattern of gas displacement by water injection will be beneficial to the scientific and rational application of water displacement in engineering. Previous studies on methane gas displacement by water injection in coal seams only focused on the effect of water displacement on the methane desorption pattern, and a fixed volume of water was used in the experiments to represent the on-site flowing water displacement environment, which widened the gap between the experimental environment and the on-site environment. In view of this, an independently designed two-phase displacement test device was used to conduct experiments of coal seam water injection to displace methane gas under different water injection pressures, and the pattern of displacing methane gas by coal seam water injection was analyzed. The results of this study can provide theoretical guidance for coal seam water injection to control gas disasters.

2. Materials and Methods

2.1. Coal Sample Preparation. The coal samples used for the test were taken from Coal Seam II₁ of the 11th Mine of Pingdingshan Tianan Coal Mining Co., Ltd. in Pingdingshan City, Henan Province. Coal Seam II₁ was identified as an outburst coal seam. The physical parameters of coal which were evaluated using Chinese national standards are shown in Table 1. Due to the softness of the coal at the sampling site, coal briquette was used for the test. A crusher was used to crush the collected coal, and a standard sieve was used to screen out coal powder with particle sizes of 0.25–0.38 mm. Then, water was utilized as a binder to mix the powder evenly before the mixed powder was placed into a briquette preparation device. Finally, a pressure of 100 MPa was applied to the briquette preparation device for 30 min, producing 3 coal samples with 50 mm in diameter and about 100 mm in

length. The coal samples were placed in a drying oven at 60°C for 24 h.

2.2. Test Device. The two-phase displacement test device is shown in Figure 1. The test device consists of an adsorption equilibrium system, a vacuum system, a temperature control system, a water injection system, a loading system, and a gas collection system. The adsorption equilibrium system includes an adsorption tank, a gas storage tank, and a pressure control valve. The pressure regulating range of the pressure control valve is 0–2.5 MPa. The vacuum system includes a vacuum pump and a vacuum gauge. The temperature control system includes a temperature controller and a water bath tub. The water injection system includes a constant-flux pump and a one-way valve. The maximum water injection pressure of the constant-flux pump is 40 MPa. The loading system includes an axial hydraulic loading device and a lateral hydraulic loading device. The gas collection system includes a gas-liquid separation bottle and a gas collection cylinder.

Figure 2 shows a simplified model of coal seam water injection. Water continuously flows into the coal body from the hole under pressure. With the increase in water injection time, the wetting radius continues to expand. The water first passes through the coal body near the water injection area, so that the coal body near the water injection area is seeped for a prolonged period. However, the time the water takes to reach the coal body far from the water injection area is long, and the time for the coal body far from the water injection area to be seeped through by water is short [27]. Thus, the distance from the coal body to the water injection hole dictates the length of time that the water displacement of gas lasts in the coal body. While the water flows through the coal, the pressure of the water flow gradually decreases. Therefore, the coal body within the wetting radius of the water is under a different water seepage time and water injection pressure. The two-phase displacement test device shown in Figure 1 controls the pressure and water injection time at both ends of the coal sample through a constant-flux pump and a pressure control valve, which can be used to simulate the displacement of adsorbed methane by flowing water in different areas within the water injection wetting radius.

2.3. Test Process. Coal seam water injection displacing methane tests were conducted under the same adsorption equilibrium pressure but different water injection pressures. To place the coal body under a stable adsorption pressure, the pressure at the exhaust (liquid) end during the water injection process is equal to the adsorption equilibrium pressure of the coal sample. The specific test procedures are as follows:

- (1) Checking the airtightness of the device. Gauze was placed at both ends of the coal sample to prevent the coal fragments from blocking the device pipelines during the water injection process. The coal sample was coated with silicone laterally, wrapped in heat shrinkable sleeves after drying, and placed in the adsorption tank. The coal sample was subjected to an axial pressure and confining pressure

TABLE 1: Physical parameters of coal sample.

Physical parameters	Moisture (%)	Ash content (%)	Volatile matter (%)	True relative density (cm ³ /g)	Apparent relative density (cm ³ /g)	Porosity (%)
Value	1.38	20.27	30.97	1.43	1.34	6.29

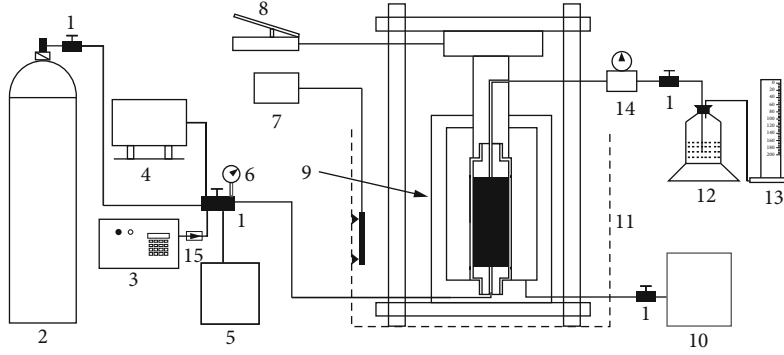


FIGURE 1: The two-phase displacement test device. 1: valve; 2: gas cylinder; 3: constant-flux pump; 4: vacuum pump; 5: gas storage tank; 6: pressure gauge; 7: temperature controller; 8: hydraulic oil pump; 9: adsorption tank; 10: hydraulic water pump; 11: water bath tub; 12: gas-liquid separation bottle; 13: gas collection cylinder; 14: pressure control valve; 15: one-way valve.

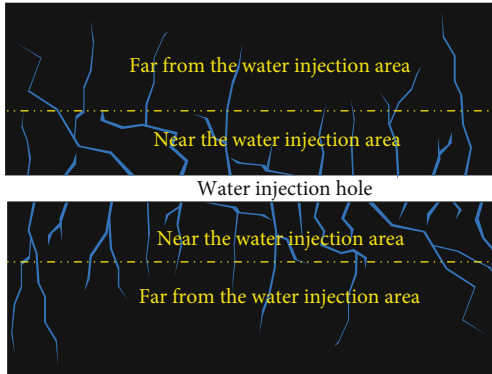


FIGURE 2: Simplified model of coal seam water injection.

of 8 MPa. High-pressure helium gas was injected to check that the device was airtight

- (2) Measurement of the free space volume. First, a steel column with 50 mm in diameter and 100 mm in length was used to replace the coal sample to measure the volume of the pipeline at both ends of the coal sample and the total volume of the gas storage tank and the connecting pipeline. After installing the coal sample, the free space volume of the coal sample was measured using helium
- (3) Gas adsorption. The adsorbed gas was methane with a purity of 99.99%. First, vacuum degassing was implemented on the test device with a vacuum degree less than 10 Pa. After completing degassing, the gas storage tank was filled with methane gas, and the stable pressure of the gas storage tank was p_1 . The pressure control valve was adjusted so that

its opening pressure was greater than p_1 . The intake valve of the adsorption tank was opened, which was connected with the gas storage tank. The temperature of the water bath outside the adsorption tank was set to 20°C. The adsorption time of the first group of coal samples was 6 h. Then, the adsorption of each group of coal samples was stopped when the adsorption equilibrium pressure was equal to that of the first group of coal samples. The volume V_1 of the methane gas entering the adsorption tank is expressed by the following equation:

$$V_1 = \frac{273.15(p_1 - p_2)}{0.10325T_0} V_2, \quad (1)$$

where p_2 refers to the adsorption equilibrium pressure of the coal sample, with a value of 0.60 MPa; V_2 stands for the total volume of the gas storage tank and the connecting pipeline, mL; and T_0 represents the temperature of the test chamber, K.

- (4) Gas desorption. The opening pressure of the pressure control valve was quickly adjusted to 0 MPa, and the gas desorption test was started. The desorption test was stopped when the gas output was less than 0.1 mL/min. In other studies, the authors conducted natural desorption tests of multiple groups of coal samples under exactly the same conditions, and the desorption data of each group of coal samples differed slightly. Therefore, only the natural desorption test of coal samples with a water injection pressure of 4 MPa was conducted in this study. For comparative analysis, the desorbed gas is converted to the volume in the standard state

$$V_4 = \frac{273.15(p_0 - p_s)}{0.10325T_0} V_3, \quad (2)$$

where V_3 refers to the volume of the desorption gas recorded in the experiment, mL; V_4 stands for the volume of desorption gas in the standard state, mL; p_0 represents the laboratory air pressure, MPa; and P_s is the saturated steam pressure, MPa.

- (5) Water injection displacement. Step (3) was repeated. When the adsorption equilibrium pressure of the coal sample reached p_2 , the valve between the adsorption tank and the gas storage tank was closed, and the opening pressure of the pressure control valve was set to p_2 . After turning the constant-flux pump on, 7 mL of distilled water was injected first and then turned off, and the gas in the pipeline at the inlet end was discharged to reduce the influence from the gas in the pipeline. When the gas pressure in the adsorption tank dropped to p_2 , the water injection pressure of the constant-flux pump was set to 4 MPa. The constant-flux pump was turned on again, and the water injection was stopped when the volume of gas discharged from the adsorption tank was less than 0.1 mL/min. The valve at the water inlet end of the adsorption tank was closed, the opening pressure of the pressure control valve was adjusted to 0 MPa, and depressurization and desorption were conducted on the coal sample.
- (6) Device cleaning. The coal sample was disassembled, and the residual water in the pipeline was cleaned. Then, the next set of tests was conducted after replacing the coal sample with a new one.

3. Results

3.1. Moisture Content of the Coal Samples. Table 2 shows the change in the moisture content of the coal samples after the methane displacement test with distilled water injected under different pressures. The moisture content of the coal samples is directly proportional to the water injection pressure, but the differences in the moisture content of coal samples under different water injection pressures are small. The coal samples were injected with water for an extended period of time; the coal samples were fully wet, and the moisture content of each group of coal samples reached the saturated state. At this time, the water injection pressure has little effect on the moisture content of the coal sample.

3.2. Ratio of Displaced Methane. The volume of displaced methane per unit mass of the coal sample is denoted as the ratio of displaced methane. Figure 3 reveals that as the water injection pressure increases, the ratio of displaced methane increases. The increasing rate of methane displacement under different water injection pressures decreases slowly as the displacement time increases. Before water is discharged from the discharging end of the adsorption tank (the stage without water discharge), methane gas is dis-

TABLE 2: Moisture content of the coal samples.

Water injection pressure/MPa	Adsorption equilibrium pressure/MPa	Moisture content/%
2	0.60	11.5
4	0.60	11.6
6	0.60	11.8

charged continuously from the discharging end. The methane gas in the stage without water discharge primarily comes from the free gas in the pores and cracks of the coal sample and the pipeline at the discharging end of the coal sample. When the water enters the coal sample from one end of the coal sample, it squeezes the free gas in the pores and cracks so that the gas pressure at the front end of the water flow increases. A gas pressure gradient is generated in the coal sample, causing the methane gas to seep in the direction of the water flow. The greater the water flow rate is, the greater the pressure gradient of the gas generated in the coal sample, and the greater the volume of gas discharged from the discharge end. The water flow rate is positively correlated with the water injection pressure. Therefore, the greater the water injection pressure is, the greater the volume of discharged gas at the stage without water discharge.

When water is discharged (the stage that discharges the water-gas mixture), the volume of discharged gas rapidly decreases, which is reflected by the decrease in the slope of the change curve of methane displacement, as shown in Figure 3. A smaller water injection pressure leads to a greater change in the slope. At the stage with the discharge of the water-gas mixture, the gas discharged from the coal body with the water flow comes from the free gas in the dry area and the displaced gas in the wet area. Under the same displacement time, the ratio of displaced methane increases with the increase in the water injection pressure, indicating that the volume of discharged gas is also positively correlated with the water flow rate at the water-gas mixture discharge stage. The water flow rates of coal samples with water injection pressures of 2 MPa, 4 MPa, and 6 MPa are approximately 0.70 g/min, 2.01 g/min, and 3.03 g/min, respectively. When the water injection pressure is 2 MPa, the water flow rate of the coal sample differs greatly from that of the other coal samples, while the difference between the water flow rate of the coal sample with a water injection pressure of 4 MPa and that with a water injection pressure of 6 MPa is relatively small. The trend of the water flow rate with the water injection pressure is the same as that of the ratio of displaced methane with the water injection pressure, which confirms that the volume of discharged gas is directly proportional to the water flow rate.

After the displacement is stopped, the methane desorption quantity of coal samples with water injection pressure of 2 MPa, 4 MPa, and 6 MPa is 0.18 mL/g, 0.28 mL/g, and 0.11 mL/g, respectively, which is much smaller than the desorption quantity of nonwater-injected coal samples at the same adsorption equilibrium pressure, as shown in Figure 4. This is due to the large amount of gas being

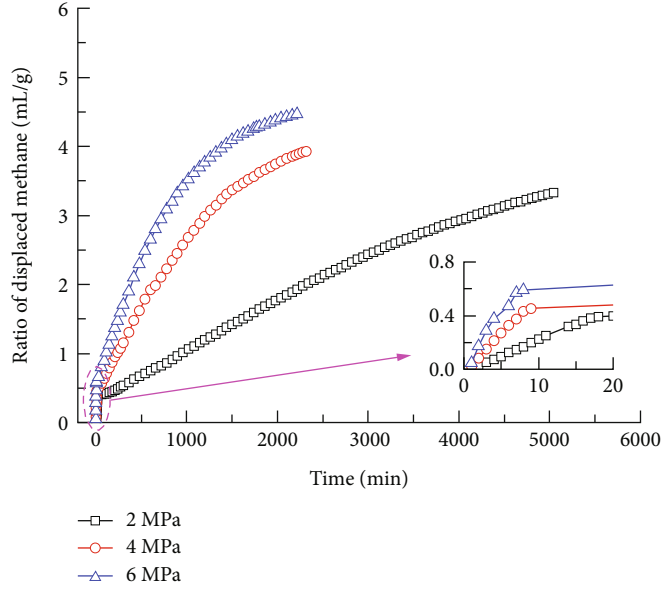


FIGURE 3: Ratio of displaced methane under different water injection pressures.

displaced after a long period of displacement and the blocking effect of the retention water, which makes the desorption quantity after the cessation of displacement much lower.

3.3. *Displacement Rate and Water Displacement Rate.* The volume of gas discharged per unit of displacement time is denoted as the displacement rate (DR), expressed as follows:

$$v_t = \frac{q_t}{\Delta t}, \quad (3)$$

where v_t refers to the DR, mL/min; Δt represents the displacement time, min; and q_t stands for the volume of gas discharged during the displacement time Δt , mL.

The ratio of the volume of gas discharged at the discharge end of the adsorption tank to the mass of water injected in the corresponding displacement time is denoted as the water displacement rate (WDR). At the initial stage of coal sample water injection, the water flow rate fluctuates greatly, and the estimated water mass is used to calculate the WDR:

$$v_w = \frac{q_t}{q_w}, \quad (4)$$

where v_w refers to the WDR, mL/g; q_w stands for the mass of water injected during the displacement time Δt , g.

Figures 5 and 6 show the change patterns of DR and WDR with displacement time under different water injection pressures, respectively. The DR and the WDR have the same change pattern. At the stage without water discharge, the DR and WDR can be divided into an increasing stage and a stable stage. After displacement starts, the water injection pressure increases rapidly, then fluctuates around the set water injection pressure value and gradually stabilizes to the water injection pressure value. The volume of dis-

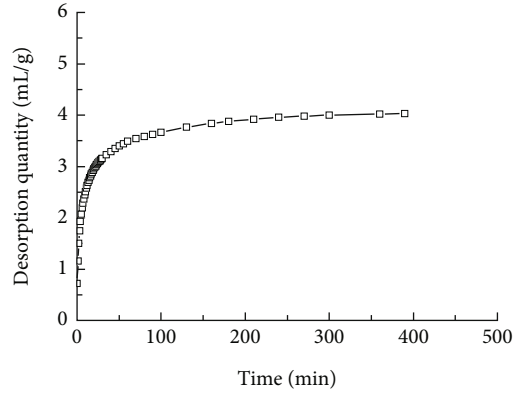


FIGURE 4: Gas desorption quantity from nonwater-injected coal sample (including the gas in the pipeline).

charged gas is positively correlated with the water injection pressure. Therefore, the DR increases with the increase in the water injection pressure at the stage without water discharge. However, the short duration of this stage and the gas discharged mainly from the gas in the discharging end of the pipeline make the WDR under different water injection pressures differed slightly in the stable stage.

A dominant path is present for coal sample water injection. Water first flows along the dominant path with low resistance and then slowly enters the pores and cracks outside the dominant path [31, 32]. This makes the coal sample not sufficiently wet after entering the water-gas mixture discharge stage, but the gas in the pipeline has been discharged. Therefore, all the discharged gas in this stage comes from the coal sample. However, due to the high resistance of discharging the gas from the coal sample, only a small amount of gas is discharged, causing the DR and WDR to be greatly reduced, as shown in Figures 4 and 5. In the water-gas mixture discharge

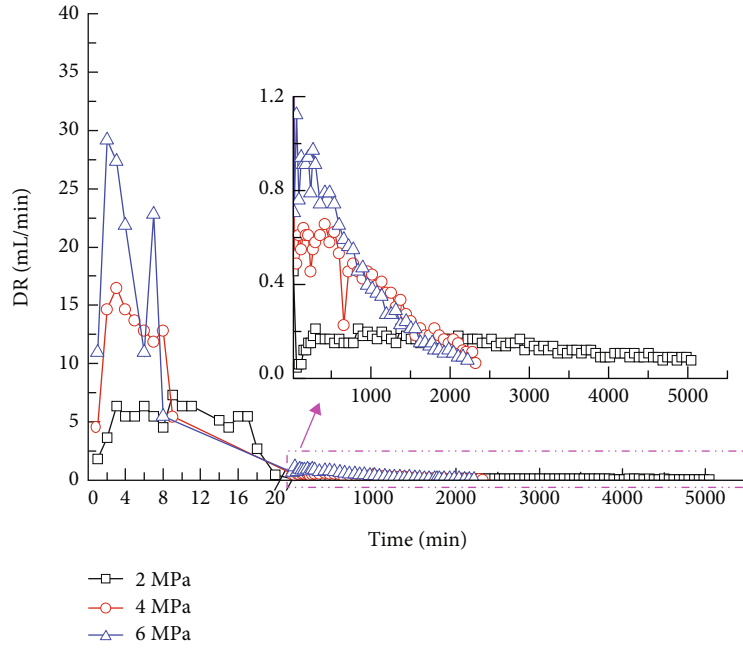


FIGURE 5: DR under different water injection pressures.

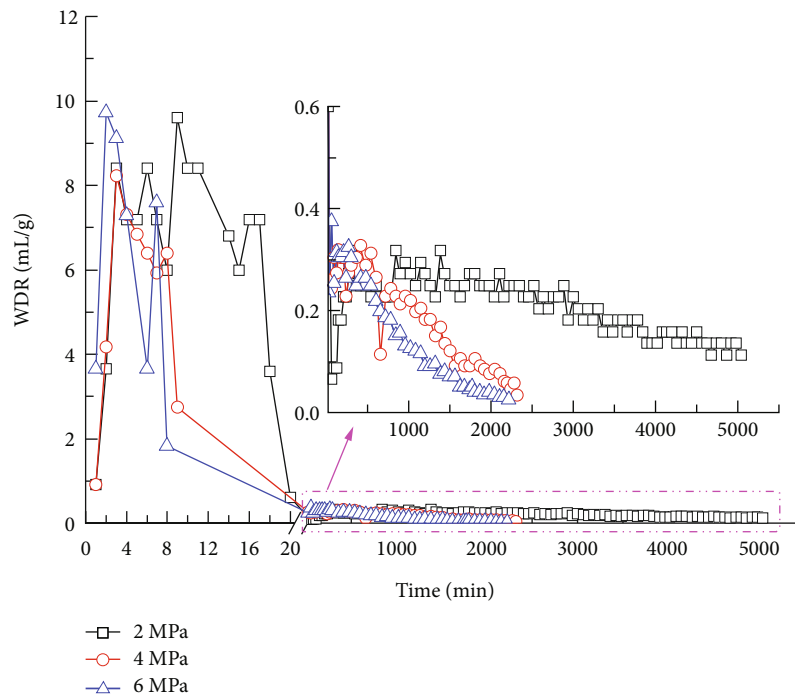


FIGURE 6: WDR under different water injection pressures.

stage, the DR and WDR can be divided into stable and attenuation stages. In the stable stage, the higher the injection pressure, the faster the water moves in the pore fissure and the greater the amount of displaced gas, causing the DR in the stable stage to increase with the injection pressure. The WDR, on the other hand, does not vary significantly with the injection pressure, indicating that the amount of gas released per unit of water in the stable stage is unrelated to the injection pres-

sure. When the coal sample is nearly fully wet, all the discharged gas comes from the displaced gas. When the wet area stops expanding, the increasing rate of the volume of displaced gas gradually decreases [27, 33]. The DR and WDR enter the attenuation stage. During the early stages of displacement, the volume of discharged gas increases with the increase in the water injection pressure, resulting in a rapid decrease in the methane content of the coal sample. The volume of

displaced gas decreases as the methane content of the coal sample decreases, and thus, a higher water injection pressure creates faster attenuation of the DR and WDR in the attenuation stage.

At the attenuation stage of the water-gas mixture discharge stage, a higher water injection pressure creates faster attenuation of the DR and WDR. During the early stages of displacement, the volume of discharged gas increases with the increase in the water injection pressure, resulting in the rapid decrease in the methane content of the coal sample. The volume of displaced gas decreases with the decrease in the methane content of the coal sample, and the DR and WDR of the coal sample with a high water injection pressure exhibit a faster attenuation at the attenuation stage, as shown in Figures 5 and 6.

3.4. Methane Displacement Time. The time when the displacement test reaches the set stopping condition is used as the displacement time of the coal sample. Figure 7 indicates that the displacement time decreases with the increase in the water injection pressure. When the water injection pressure increases from 2 MPa to 4 MPa, the displacement time is decreased by 54.0%, while when the water injection pressure increases from 4 MPa to 6 MPa, the displacement time is decreased by only 4.3%, indicating that there is a critical water injection pressure under the set test stop condition. Continuously increasing the water injection pressure after exceeding the critical water injection pressure does not improve the displacement efficiency. When the water injection pressure is lower than the critical water injection pressure, the displacement time decreases rapidly with the increase in the water injection pressure, while when the water injection pressure is greater than the critical water injection pressure, the displacement time does not change appreciably with the increase in the water injection pressure.

3.5. Methane Displacement Rate. The ratio of the volume of methane displaced from unit mass of the coal sample to the methane content of the coal sample is denoted as the methane displacement rate, expressed as follows:

$$\eta_1 = \frac{q_1}{Q} \times 100\%, \quad (5)$$

where η_1 refers to the methane displacement rate, %; q_1 represents the volume of methane displaced from unit mass of the coal sample, mL/g; and Q represents the methane content of the coal sample, mL/g.

The ratio of the volume of desorbed methane to the methane content of the coal sample is denoted as the natural desorption rate, expressed as follows:

$$\eta_2 = \frac{q_2}{Q} \times 100\%, \quad (6)$$

where η_2 refers to the desorption rate and q_2 denotes the volume of methane naturally desorbed from unit mass of the coal sample, mL/g.

Figure 8 indicates that with the increase in water injection pressure, the methane displacement rate increases. In

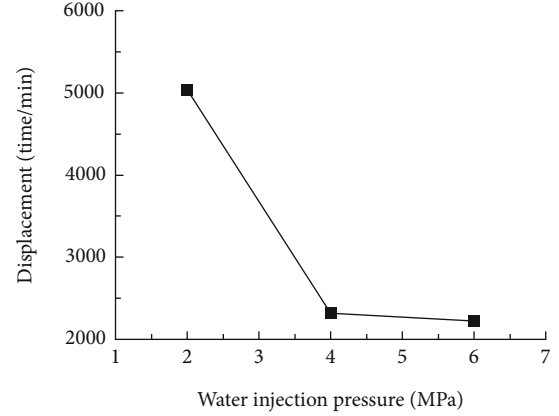


FIGURE 7: Displacement time under different water injection pressures.

the meantime, the methane displacement rate is linearly related to the water injection pressure. The natural desorption rate of the coal sample is 65.4%. The methane displacement rates of coal samples with water injection pressures of 4 MPa and 6 MPa are 66.0% and 76.3%, respectively, which are higher than the natural desorption rate. Meanwhile, the methane displacement rate of the coal sample with a water injection pressure of 2 MPa is 55.3%, which is lower than the natural desorption rate. Figures 4 and 5 reveal that the water flow rate of the coal sample with a water injection pressure of 2 MPa is small, resulting in small values and slow attenuation of the DR and WDR at the water-gas mixture discharge stage. If water is continuously injected, a certain volume of gas will still be discharged from the coal sample. The final methane displacement rate is likely to be greater than the natural desorption rate. Based on the above analysis, coal seam water injection can promote the desorption of the adsorbed gas, so that a large amount of adsorbed methane gas is displaced.

4. Discussion

The test results above indicate that the higher the water injection pressure is, the more rapidly the ratio of displaced methane increases, and the shorter the displacement time is. The DR increases with the increase in the water injection pressure at the stage without water discharge, while the WDR under different water injection pressures differed slightly; at the later stage of water injection, the higher the water injection pressure is, the faster the attenuation. According to the fact that the methane displacement rate under different water injection pressures is high and greater than the natural desorption rate, water injection promotes methane desorption and can displace a large amount of adsorbed gas in the coal.

When the gas pressure is less than 8 MPa, the solubility of methane in water has a linear relationship with the gas pressure [34]. The calculation formula for the solubility of methane in water at 20°C and a gas pressure of 0-3 MPa is given:

$$s = 0.3152p_2, \quad (7)$$

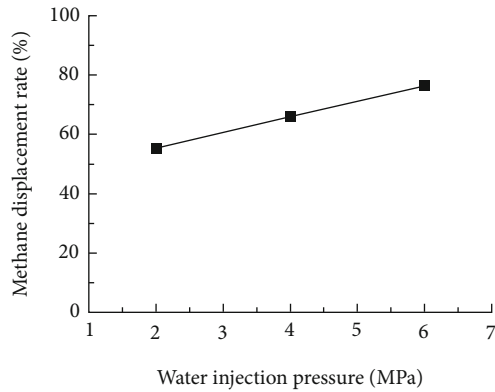


FIGURE 8: Methane displacement rate under different water injection pressures.

where s refers to the solubility, L/L and p_z represents the gas pressure, MPa.

According to the calculation formula, when the methane gas pressure is 2-6 MPa, the solubility of methane in water is 0.63-1.89 L/L. The solubility of methane is quite large under the test conditions, which greatly influences the displacement pattern. Coal is a porous medium with complex pores and fissures [35]. According to the study, porous medium easily form confined gas during the process of water driven gas [36, 37]. In particular, the small pores where water is not easily entered are the main places for gas adsorption in coal [38]. This causes a large amount of gas to be difficult to drive out. Considering gas solubility, the blocked methane gas is dissolved in water at the water-gas interface, which reduces the pressure in the gas zone. According to the Langmuir adsorption theory, methane desorption occurs in the gas zone, but the desorbed methane is not enough to restore the pressure in the gas zone [39]. The equilibrium state of forces at the water-gas interface is broken. Assuming that the water-gas interface can move under the action of force, methane gas dissolution will promote the continuous movement of the water-gas interface until it occupies the entire gas zone. If the force at the water-gas interface cannot move the water-gas interface, the gas concentration at the water-gas interface decreases due to gas dissolution at the water-gas interface, while the gas concentration far away from the water-gas interface is high, forming a concentration gradient in the gas zone. According to Fick's law of diffusion, methane gas undergoes a diffusion motion [40]. Under methane gas dissolution, diffusion, and desorption, the gas content in the pores gradually decreases. The methane gas dissolved in water is discharged with flowing water. In the pore fractures occupied by water, the adsorbed gas is displaced by water, and the displaced gas dissolves in water or forms bubbles in the water, which is then taken out by the water flow. Finally, a large amount of methane gas in the coal samples is displaced by prolonged flowing water injection.

According to the analysis, the method of using water injection to displace methane can reduce the gas content of the coal. The test results also explain the existence of areas with increased gas content and those with decreased gas

content after water injection in the field. The increase in gas content in local areas increases the risk of coal and gas outbursts [18]. Therefore, disasters caused by methane displacement should be considered when using coal seam water injection to control gas disasters. Briquettes are used in this study for displacement tests, and there are certain differences between briquettes and raw coal in properties and structures that may affect the displacement pattern.

5. Conclusions

In this paper, a two-phase displacement test device was used to conduct an experiment on displacing methane under different water injection pressures, thereby analyzing the change patterns of the displacement volume, DR and WDR, displacement time, and methane displacement rate in addition to the influence of methane solubility in water on displacement patterns. The following important conclusions were drawn:

- (1) A greater water injection pressure leads to a greater water flow rate and a greater volume of methane gas flushed out by the discharged water. The DR increases with the increase in the water injection pressure at the stage without water discharge, while the WDR under different water injection pressures differed slightly. At the later stage of displacement, a higher water injection pressure causes the DR and WDR of the coal sample to attenuate faster
- (2) According to the change pattern of the displacement time, there is a critical water injection pressure for coal seam water injection. When the water injection pressure is less than the critical water injection pressure, the displacement time decreases rapidly with the increase in the water injection pressure, while when the water injection pressure is greater than the critical water injection pressure, the change in the displacement time with the water injection pressure is no longer evident
- (3) Due to the high solubility of methane gas in water under high pressure, gas that does not typically discharge from the coal is discharged due to the dissolution of methane in water, so that the displacement of methane by water injection has a large methane displacement rate, and a greater water injection pressure leads to a higher methane displacement rate

Data Availability

The data used to support the findings of this study are available from the corresponding author upon request.

Conflicts of Interest

The authors declare that there is no conflict of interest regarding the publication of this paper.

Acknowledgments

This study was funded by the National Key R&D Program of China (no. 2017YFC0804208).

References

- [1] P. Zhang, F. Li, H. Zhu, H. Niu, and X. Li, "Statistical analysis and prevention countermeasures of coal mine accidents from 2008 to 2020," *Mining Safety and Environmental Protection*, vol. 49, pp. 128–134, 2022.
- [2] C. Zhang, E. Wang, J. Xu, and S. Peng, "A new method for coal and gas outburst prediction and prevention based on the fragmentation of ejected coal," *Fuel*, vol. 287, p. 119493, 2021.
- [3] Q. Hu, S. Zhang, G. Wen, L. Dai, and B. Wang, "Coal-like material for coal and gas outburst simulation tests," *International Journal of Rock Mechanics and Mining Sciences*, vol. 74, pp. 151–156, 2015.
- [4] M. Wold, L. Connell, and S. Choi, "The role of spatial variability in coal seam parameters on gas outburst behaviour during coal mining," *International Journal of Coal Geology*, vol. 75, no. 1, pp. 1–14, 2008.
- [5] Q. Yao, T. Chen, M. Ju, S. Liang, Y. Liu, and X. Li, "Effects of water intrusion on mechanical properties of and crack propagation in coal," *Rock Mechanics and Rock Engineering*, vol. 49, no. 12, pp. 4699–4709, 2016.
- [6] R. Qian, G. Feng, J. Guo, P. Wang, X. Wen, and C. Song, "Experimental investigation of mechanical characteristics and cracking behaviors of coal specimens with various fissure angles and water-bearing states," *Theoretical and Applied Fracture Mechanics*, vol. 120, p. 103406, 2022.
- [7] X. Liu, G. Xu, C. Zhang et al., "Time effect of water injection on the mechanical properties of coal and its application in rockburst prevention in mining," *Energies*, vol. 10, no. 11, p. 1783, 2017.
- [8] Q. Yao, C. Zheng, C. Tang, Q. Xu, Z. Chong, and X. Li, "Experimental investigation of the mechanical failure behavior of coal specimens with water intrusion," *Frontiers in Earth Science*, vol. 7, p. 348, 2020.
- [9] R. Shen, H. Li, E. Wang et al., "Mechanical behavior and AE and EMR characteristics of natural and saturated coal samples in the indirect tensile process," *Journal of Geophysics and Engineering*, vol. 16, no. 4, pp. 753–763, 2019.
- [10] Z. Liu, K. Sheng, H. Yang, W. Su, P. Hu, and B. Dong, "Numerical simulation study and application of coal seepage evolution law around water injection borehole in the stope "dynamic-static" pressure zone," *Measurement*, vol. 195, p. 111107, 2022.
- [11] W. Yang, M. Lin, G. Walton et al., "Blasting-enhanced water injection for coal and gas out-burst control," *Process Safety and Environmental Protection*, vol. 140, pp. 233–243, 2020.
- [12] X. Li, D. Chen, Y. Zhou, Y. Kang, X. Meng, and X. Zhang, "The influence of fracturing fluid on CBM desorption-diffusion-seepage capacity of coal," in *SPE/IATMI Asia Pacific Oil & Gas Conference and Exhibition*, Nusa Dua, Bali, Indonesia, October 2015.
- [13] Z. Pan, L. D. Connell, M. Camilleri, and L. Connelly, "Effects of matrix moisture on gas diffusion and flow in coal," *Fuel*, vol. 89, no. 11, pp. 3207–3217, 2010.
- [14] M. B. D. Aguado and C. G. Nicieza, "Control and prevention of gas outbursts in coal mines, Riosa-Olloniego coalfield, Spain," *International Journal of Coal Geology*, vol. 69, no. 4, pp. 253–266, 2007.
- [15] Y. Xu and L. Wang, "Technical parameters of hydraulic punching in a typical coal seam and an investigation of outburst prevention effect: a case study in the Machi mine, China," *Geotechnical and Geological Engineering*, vol. 38, no. 2, pp. 1971–1986, 2020.
- [16] F. Hao, M. Liu, and W. Zuo, "Coal and gas outburst prevention technology and management system for Chinese coal mines: a review," in *Mine Planning and Equipment Selection*, pp. 581–600, Springer, 2014.
- [17] V. Hudecek, "Analysis of safety precautions for coal and gas outburst-hazardous strata," *Journal of Mining Science*, vol. 44, no. 5, pp. 464–472, 2008.
- [18] W. Yang, C. Lu, G. Si, B. Lin, and X. Jiao, "Coal and gas outburst control using uniform hydraulic fracturing by distress blasting and water-driven gas release," *Journal of Natural Gas Science and Engineering*, vol. 79, p. 103360, 2020.
- [19] Z. Wang, W. Su, X. Tang, and J. Wu, "Influence of water invasion on methane adsorption behavior in coal," *International Journal of Coal Geology*, vol. 197, pp. 74–83, 2018.
- [20] B. Huang, W. Lu, S. Chen, and X. Zhao, "Experimental investigation of the functional mechanism of methane displacement by water in the coal," *Adsorption Science & Technology*, vol. 38, no. 9–10, pp. 357–376, 2020.
- [21] J. Wu, J. Yu, Z. Wang, X. Fu, and W. Su, "Experimental investigation on spontaneous imbibition of water in coal: implications for methane desorption and diffusion," *Fuel*, vol. 231, pp. 427–437, 2018.
- [22] X. Chen, W. Shan, R. Sun, and L. Zhang, "Methane displacement characteristic of coal and its pore change in water injection," *Energy Exploration & Exploitation*, vol. 38, no. 5, pp. 1647–1663, 2020.
- [23] W. Lu, B. Huang, S. Chen, and X. Zhao, "Experimental verification of the water-methane displacement effect in gassy coal," *International Journal of Oil, Gas and Coal Technology*, vol. 23, no. 1, pp. 126–141, 2020.
- [24] G. Ni, B. Lin, C. Zhai, Q. Li, S. Peng, and X. Li, "Kinetic characteristics of coal gas desorption based on the pulsating injection," *International Journal of Mining Science and Technology*, vol. 24, no. 5, pp. 631–636, 2014.
- [25] P. Li, F. Du, F. Wang, P. Zhang, Y. Jiang, and B. Cui, "Influence of water injection on the desorption characteristics of coalbed methane," *Energy Science & Engineering*, vol. 8, no. 12, pp. 4222–4228, 2020.
- [26] K. Zhang, Y. Cheng, L. Wang, J. Dong, C. Hao, and J. Jiang, "Pore morphology characterization and its effect on methane desorption in water-containing coal: an exploratory study on the mechanism of gas migration in water-injected coal seam," *Journal of Natural Gas Science and Engineering*, vol. 75, p. 103152, 2020.
- [27] B. Huang, Q. Cheng, and S. Chen, "The verification of displacement methane effect caused by hydraulic fracturing in gassy coal seams," *Arabian Journal of Geosciences*, vol. 11, no. 20, pp. 1–14, 2018.
- [28] A. Busch and Y. Gensterblum, "CBM and CO₂-ECBM related sorption processes in coal: a review," *International Journal of Coal Geology*, vol. 87, no. 2, pp. 49–71, 2011.
- [29] M. Mukherjee and S. Misra, "A review of experimental research on enhanced coal bed methane (ECBM) recovery via CO₂ sequestration," *Earth-Science Reviews*, vol. 179, pp. 392–410, 2018.
- [30] X. Qin, H. Singh, and J. Cai, "Sorption characteristics in coal and shale: a review for enhanced methane recovery," *Capillarity*, vol. 5, no. 1, pp. 1–11, 2022.

- [31] J. Zhang, C. Wei, V. Vandeginste et al., “Experimental simulation study on water migration and methane depressurizing desorption based on nuclear magnetic resonance technology: a case study of middle-rank coals from the Panguan syncline in the western Guizhou region,” *Energy & Fuels*, vol. 33, no. 9, pp. 7993–8006, 2019.
- [32] Y. Pan, J. Tang, and C. Li, “NMRI test on two-phase transport of gas-water in coal seam,” *Diqiu Wuli Xuebao*, vol. 51, 2008.
- [33] D. Zhao, Y. Zhao, and Z. Feng, “Laboratory experiment on coalbed-methane desorption influenced by water injection and temperature,” *Journal of Canadian Petroleum Technology*, vol. 50, no. 7, pp. 24–33, 2011.
- [34] A. Chapoy, A. H. Mohammadi, D. Richon, and B. Tohidi, “Gas solubility measurement and modeling for methane-water and methane-ethane-n-butane-water systems at low temperature conditions,” *Fluid Phase Equilibria*, vol. 220, no. 1, pp. 113–121, 2004.
- [35] D. Ye, G. Liu, F. Gao, R. Xu, and F. Yue, “A multi-field coupling model of gas flow in fractured coal seam,” *Advances in Geo-Energy Research*, vol. 5, no. 1, pp. 104–118, 2021.
- [36] Z. L. Li DW and K. Zhou, “Gas-water two-phase flow mechanism in visual microscopic poremode,” *Journal of China University of Petroleum*, vol. 32, no. 3, pp. 80–83, 2008.
- [37] L. Sima, C. Wang, L. Wang, F. Wu, L. Ma, and Z. Wang, “Effect of pore structure on the seepage characteristics of tight sandstone reservoirs: a case study of Upper Jurassic Penglaizhen Fm reservoirs in the western Sichuan Basin,” *Natural Gas Industry B*, vol. 4, no. 1, pp. 17–24, 2017.
- [38] R. Baouche and D. A. Wood, “Characterization and estimation of gas-bearing properties of Devonian coals using well log data from five Illizi Basin wells (Algeria),” *Advances in Geo-Energy Research*, vol. 4, no. 4, pp. 356–371, 2020.
- [39] Y. Meng, D. Tang, Y. Qu, H. Xu, and Y. Li, “Division of the stages of coalbed methane desorption based on the Langmuir adsorption isotherm,” *Arabian Journal of Geosciences*, vol. 8, no. 1, pp. 57–65, 2015.
- [40] B. P. Van Milligen, P. Bons, B. A. Carreras, and R. Sanchez, “On the applicability of Fick’s law to diffusion in inhomogeneous systems,” *European Journal of Physics*, vol. 26, no. 5, pp. 913–925, 2005.